# Microwave-assisted and conventional hydrothermal carbonization of lignocellulosic waste material: Comparison of the chemical and structural properties of the hydrochars

**Sunday E. Elaigwu[a,b]*, Gillian M. Greenway[a]**

**[a]Department of Chemistry, University of Hull, Cottingham Road, Hull, HU6 7RX, UK**

**[b]Department of Chemistry, University of Ilorin, PMB 1515, Ilorin, Kwara State, Nigeria**

**Corresponding author. Tel. +44 7733680543; fax: +44 1482466410**

**Email addresses: S.E.Elaigwu@2009.hull.ac.uk, sunnietrinex@hotmail.com**

## Abstract

This study compares the chemical and structural properties of the hydrochars prepared from microwave-assisted and conventional hydrothermal carbonizations of *Prosopis africana* shell, a waste plant material. The preparation involved heating the raw material in de-ionized water at 200 °C for 5-20 min, and 120-240 min in the microwave and conventional oven respectively. The prepared hydrochars were characterized using the scanning electron microscope, nitrogen sorption measurement, Fourier transform infrared spectroscopy, CHN analyzer, thermogravimetric analysis, and nuclear magnetic resonance. The results showed that the microwave-assisted hydrothermal carbonization process is fast in the carbonization of the *Prosopis africana* shell as shown by the level of conversion attained within the short time. This study presents new data on the comparison of the hydrochars from microwave-assisted and conventional hydrothermal carbonization processes of the same lignocellulosic material in terms of their properties.

**Keywords: Microwave, hydrothermal carbonization, carbonized material, *Prosopis africana* shell**

## 1. Introduction

Various methods exist for the preparation of carbonaceous materials from waste biomasses, with the aim of managing, sequestering carbon, and converting the waste materials into useful products that can find application in the environment, separation science, catalysis, and as electrode material [1]. One of such methods is the

environmentally friendly hydrothermal carbonization process, which involves the heating of biomass under pressure in water at about 180-200 °C to form char called hydrochar, and water-soluble organic substances [2,3]. Thus, in the hydrothermal carbonization process the stored energy in the biomass is used more efficiently. It is an important process because water acts as both the reagent and reactive environment, and it has been applied in the synthesis of different types of carbonaceous materials [4].

Microwave technology has been shown to be more energy efficient than conventional methods of heating in many applications, because it provides selective, fast and homogenous heating, which reduces processing time and costs significantly [5,6]. As such it can be an attractive alternative to the conventional method of hydrothermal carbonization of waste materials. Hydrothermal carbonization process was first reported in 1913 by Bergius and Specht [7], and has been proven to be a promising and a sustainable waste management method. The ultimate goal of the process is to convert waste materials into value-added products, while promoting the integration of the carbon formed in the solid-phase. Several other researches have been carried out over the years using conventional and microwave heating to produce valuable products, from different kinds of materials, for various applications [8-17]. Despite all these studies, a direct comparison of the solid product (hydrochar) obtained from the microwave-assisted and conventional hydrothermal carbonization methods of the same lignocellulosic material has not been reported to the best of our knowledge. Therefore, in this study we made comparisons between the hydrochars prepared from a waste plant material (*Prosopis africana* shell) using these methods, with focus on the similarities between the structural and chemical properties of the hydrochars, in order to provide useful information about the microwave-assisted and conventional oven hydrothermal carbonization processes.

The *Prosopis africana* (Mimosaceae) used in this study is a multi-purpose tree of great economic value among the rural communities in Nigeria. The shell is one of the widely available waste products obtained from it numerous uses. Detailed information on the *Prosopis africana* can be found elsewhere [18].

## 2. Materials and Methods

The *Prosopis africana* shell was collected in Benue State, Nigeria. It was crushed and sieved to 2 mm size and stored for use in the preparation of the hydrochars.

It is important to state that this study was restricted to 200 °C for safety reason based on previous report by Titirici et al., [1] that temperatures below 180 °C produces only weak or no conversions for cellulose containing materials; while temperatures exceeding 220 °C could cause a runaway of the reaction, and hydrothermal reactions at 250 °C tend to generate too much heat and pressure, which could burst the safety plate of the autoclave.

### 2.1 Preparation of the hydrochars

#### *2.1.1 Microwave-assisted hydrothermal carbonization*

This experiment was conducted in a 2.45 GHz, and 1600 W microwave oven (MARS, CEM, Milton Keynes, UK equipped with XP1500 digestion vessels). The reaction temperature was monitored with an infrared fibre optic sensor fitted into the ceramic sleeve of the reference vessel, while the reaction pressure was monitored with a pressure sensor fitted to the same reference vessel.

The procedure has been described in our previous study [18]. Briefly, 2 g of the ground *Prosopis africana* shell was weighed into a reaction vessel made of Teflon and 30 ml of de-ionized water was added to cover the solid. The reaction vessel was sealed and placed in the microwave oven. The sample was then heated at 200 °C in the microwave oven which was set to ramp to the temperature in 5 min and was held at the temperature for 5-20 min (pressure at 200 °C was about 1.80 MPa). The reaction system was allowed to cool to room temperature, and the carbonized material was filtered off using filter paper (Whatman filter paper number 3, ashless 11 cm). The hydrochar obtained was washed several times with de-ionized water until a neutral pH was reached. It was then dried in a conventional oven at 80 °C for 16 h, and stored in the desiccator for further analysis. The hydrochars were denoted as M-PAS$_{x\text{-}y}$, where x and y represent temperature (°C) and time (min) for the carbonization respectively.

### *2.1.2 Conventional hydrothermal carbonization*

This experiment was conducted in a Teflon-lined autoclave (Parr Instruments, Illinois, USA) placed in a preheated conventional oven. Experiments conducted using the same set-up to investigate the time the autoclave will take to reach the set temperature showed an average time of about 20 min.

The preparation was carried based on previous report [19]. 2 g of *Prosopis africana* shell was weighed into a Teflon-lined autoclave and 30 ml of deionized water was added. The autoclave was placed in a preheated conventional oven at 200 °C and was held for 120–240 min. The oven was allowed to cool down to room temperature and the autoclave was removed. The prepared hydrochar was filtered off with filter paper (Whatman filter paper number 3, ashless 11 cm), washed several times with deionized water until a neutral pH was obtained. It was then dried at 80 °C for 16 h, and stored in the desiccator for further analysis. The hydrochars were denoted as C-PASx-y, where x and y represent temperature (°C) and time (min) for the carbonization respectively.

## 2.2 Product yield (%)

In each case, the dry mass of the carbonized material was measured and the product yield (dry mass percentage of the raw material) was calculated as follows:

$$Product\ yield\ (\%) = \frac{Mass\ of\ carbonized\ material\ (g)}{Mass\ of\ raw\ material\ (g)} \times 100 \qquad \text{(Equation 1)}$$

## 2.3 Ash Content Determination

2 g of the carbonized material was placed into weighed ceramic crucible. The carbonized material and crucible were dried for 16 h at 80 °C and reweighed to obtain the dry carbon weight. The sample and the crucibles were then heated in a furnace at 760 °C for 6 hrs. The crucible was removed from the furnace, cooled in a desiccator and the remaining solid (ash) was weighed. Percentage ash content was calculated as follows:

$$Ash\ content\ (\%) = \frac{Remaining\ solid\ weight\ (g)}{Original\ carbon\ weight\ (g)} \times 100 \qquad \text{(Equation 2)}$$

### 2.4 pH Measurement

1 % (wt/wt) suspension of carbon material in deionized water was prepared. The pH of the suspension was measured with a pH meter (FisherBrand Hydrus 500, Fisher Scientific, Loughborough, UK), which has been calibrated with pH 4 and pH 7 buffer solutions. The calibration was confirmed by analysis of a pH 7 buffer after every five analyses and a recalibration done if the value varied by more than ± 0.1 pH units.

### 2.5 Energy properties of the hydrochars

The higher heating value (HHV) was calculated using Equation 3 as reported by Gao et al. [20]

$$HHV = 0.3383C + 1.422\,(H - O/8) \qquad \text{(Equation 3)}$$

The energy densification ratios of the hydrochars were calculated using the equation below

$$Energy\ densification\ ratio = \frac{HHV\ of\ dried\ hydrochar}{HHV\ of\ dried\ \ raw\ material} \qquad \text{(Equation 4)}$$

All experiments were carried out in triplicate, and the results are presented in Table 1.

### 2.5 Characterization Methods

The characterizations of the materials were carried out using the following instruments. The elemental analysis was carried out using Fisons instruments EA 1108 CHN analyzer. The surface areas were measured on a Micromeritics Tristar BET-$N_2$ surface area analyzer, before the analysis the samples were degassed at 120 °C for 3 h. FT-IR spectra were recorded using Thermoscientific Nicolet 380 FT-IR (Themo Scientific, Hemel Hempstead, UK), equipped with attenuated total reflectance (ATR). The morphology and particle size were visualized using a ZEISS EVO 60 SEM (Carl Zeiss, Cambridge, UK); the samples were coated with gold and platinum alloy and impregnated on a sticky disc before analysis. Thermogravimetic analysis (TGA) were carried out under $N_2$ atmosphere at a heating rate of 30 °C $min^{-1}$ using a Mettler Toledo-

TGA/DSC 1 instrument. $^{13}C$ solid-state magic angle spinning NMR experiments were carried out using a Bruker Avance II 500 MHz (11.74T) spectrometer (Bruker, Coventry, UK); the samples were packed without further treatment into a 4 mm zirconia rotor sample holder spinning at MAS rate $\nu_{MAS}$ = 8 KHz. Carbon sensitivity was enhanced using Proton-to-carbon CP MAS: recycle delay for all CP experiments was 3 s and TPPM decoupling was applied during signal acquisition. Cross polarization transfer was carried out under adiabatic tangential ramps to enhance the signal with respect to other known methods. CP time $t_{CP}$ = 500 ms. The number of transients was 200 for all the carbon samples.

## 3. Results and Discussion

### 3.1 Product yields, CHN analysis, ash, and pH content

The main objective of this work was to compare the similarity between the hydrochars (solid products) from the microwave-assisted and conventional hydrothermal carbonization of a lignocellulosic waste biomass (*Prosopis africana* shell) in terms of their product yields and properties. The results of the product yield are shown in Table 1. Despite having a longer processing time, the conventional hydrothermal process generated more or almost the same amount of product as the microwave-assisted process, which could be attributed to the amorphous cellulose activation under the irradiation with microwaves [21,22]. The product yields for the hydrochars decreased, while the carbon contents increased with increase in the processing time, due to the loss of oxygen during the increasing liquefaction and gasification reactions, which are parallel reactions to the hydrothermal process of the biomass [13,23,24].

In contrast to the carbon content, the hydrogen and oxygen contents of the hydrochars decreased with increase in the processing time. This observed trend in the hydrothermal carbonization process of biomasses has been attributed to the loss of hydrogen and oxygen due to deoxygenating, dehydration and decarboxylation reactions that occur during the hydrothermal carbonization process [25-28]. The ash content was low for the M-PAS and C-PAS because most of the inorganic compounds contained in

the *Prosopis africana* shell dissolved in water during the hydrothermal carbonization processes, while their low pH values is as a result of the high content of oxygen containing functional groups [18,29].

**Table 1**

The van Krevelen diagram (Figure 1) was also used to provide information about the transformation in the chemical structure of the raw material after carbonization, and also to qualitatively assess the carbonization process by plotting atomic ratios of H/C against O/C for the raw material and the hydrochars from both processes. The ratios of the H/C and O/C of the hydrochars decreased as the carbonization time was increased, and were lower than that of the raw material. This suggests that there was transformation during the hydrothermal carbonization processes resulting from dehydrogenation, decarboxylation, deoxygenation and dehydration reactions [8,30]. The raw *Prosopis africana* shell fell into a region that is typical for biomasses, while the hydrochars have O/C and H/C ratios akin to that of peat [31]. The graph of H/C versus O/C atomic ratios follows at diagonal line from the raw material to the hydrochars, which implies that the reaction that predominates during the hydrothermal process is dehydration reactions [30].

**Figure 1**

### 3.2 Energy properties of the hydrochars

A vital characteristic of biomass and hydrochars is their higher heating values (HHVs). It shows the total amount of energy that is present in a sample. In both processes, the HHVs calculated for the M-PAS and C-PAS increased with increase in residence time (Table 1), which is an indication of the level of carbonization attained. The HHVs of the hydrochar were similar to that of wood and paper due to lignocellulosic

nature of the raw material [19]. Hydrothermal carbonization process is associated with dehydration, decarboxylation, and condensation reactions leading to the carbonization of the raw biomass and thus resulting in energy densification, which is used to assess the effectiveness of the hydrothermal carbonization processes [19,32]. In this study, the energy densification ratios of the hydrochars are in the range of 1.24 – 1.27 and 1.12 – 1.28 for the M-PAS and C-PAS respectively, which is within the range previously reported (19,32,33].

The closeness in the properties of the M-PAS$_{200\text{-}20}$ and C-PAS$_{200\text{-}240}$ could mean that other characteristics of these hydrochars may also be comparable. Hence, further characterization will be limited to these hydrochars.

### 3.3 Chemical Characteristics

#### *ATR-FTIR Analysis*

ATR-FTIR spectroscopy was used to assess the changes in the *Prosopis africana* shell during the hydrothermal carbonization process. The FTIR spectra of the hydrochars (M-PAS$_{200\text{-}20}$ and C-PAS$_{200\text{-}240}$) shown in Figure 2a differ in intensity from that of the raw material in Figure 2b, indicating the chemical transformations that occurred when the raw material was hydrothermally carbonized. The strong presence of single bond components, such as, C-O, C-H and O-H is expected since the hydrochars were obtained from lignocellulosic biomass that contains cellulose, hemicelluloses and lignin [34]. The broad peak between 3700-3000 $cm^{-1}$ (Section 1) comes from the stretching vibration of aliphatic O-H (hydroxyl and carboxyl), while the peaks between 1200-1000 $cm^{-1}$ (Section 6) correspond to C-O stretching vibration from esters, phenols and aliphatic alcohols. The weak intensity of these peaks (Sections 1 and 6) in the hydrochars shows that dehydration and decarboxylation reactions occurred during the hydrothermal carbonization process [32]. The peak between 1800-1650 $cm^{-1}$ (Section 3) corresponds to the C=O stretching vibration of esters, carboxylic acids or aldehydes from cellulose or lignin. This peak was almost absent in the hydrochars due to the breakdown of cellulose during the hydrothermal carbonization process, while the peak between 1650-1500 $cm^{-1}$ (Section 4)

represents the C=C vibrations of the aromatic rings in lignin. This peak was still present after the carbonization process; although with reduced intensity indicating the presence of lignin fragments and intermediate structures in the hydrochars, which implies that under the conditions studied lignin did not totally breakdown [35]. The peaks between 3000-2800 $cm^{-1}$ (Section 2) are due to the stretching vibration of aliphatic C-H bonds, while the peaks between 1450-1200 $cm^{-1}$ (Section 5) are due to the bending vibration of C-H bond of the aliphatic carbons, methylene, and methyl groups indicating the presence of aliphatic structures [23]. The notable absence in the hydrochars of peaks below 1000 $cm^{-1}$ (Section 7) due to the deformation of the C-H out of plane bending vibrations is consistent with previous report [25]

**Figure 2**

***NMR Analysis***

The $^{13}C$ solid state NMR analysis of the M-$PAS_{200\text{-}20}$ and C-$PAS_{200\text{-}240}$ shown in Figure 3 provided further information on their chemical composition, and also used to confirm the functional groups present. It is usually a valuable complementary method to the FT-IR analysis in describing biomass conversion during hydrothermal carbonization process. A close comparison between the NMR spectra of the hydrochars shows very similar features. The peaks between 14–60 ppm shows the presence of aliphatic carbons, while those in the region between 100–160 ppm usually referred to as the aromatic region are all due to C=C double bond from lignin, but between 140–160 ppm are specifically due to the oxygen bound O-C=C (O-aryl) [36,37]. Due to the residual lignin, and the cellulose and hemicellulose content of the raw material, the spectra show carbohydrate resonances ($CH_2OH$ groups around 62 ppm, CHOH groups around 72 ppm, and anomeric O-C-O carbons around 90 ppm) in the O-alkyl region between 60 and 100 ppm [14,38]. The ATR-FTIR analysis has already indicated the presence of these functional groups. Therefore, the $^{13}C$ NMR and ATR-FTIR results are in good agreement with each other.

**Figure 3**

***Thermo-gravimetric analysis (TGA)***

In order to further assess the extent of conversion of the raw material under the microwave-assisted and conventional hydrothermal carbonization conditions, TGA analysis was carried out on M-PAS$_{200\text{-}20}$ and C-PAS$_{200\text{-}240}$. The TGA curve in Figure 4 showed obvious similarities in the behaviour of the hydrochars. The TGA curves can be grouped into three weight loss stages. The first stage below 200 °C where there was no significant weight loss was because the hydrothermal processes have already decomposed the components of the raw materials that would have decomposed at these temperatures. The slight loss in weight at the first stage corresponds to moisture loss and release of volatile compounds [32,39]. The second stage which occurred at about 220–410 °C, represents the temperature range at which chemical bonds begin to break and the lightest volatile compounds are released and it corresponds to the decomposition of cellulose and hemicellulose [32,40]. The third combustion stage from 410–650 °C is usually assigned to thermal degradation of lignin. Among the three components (cellulose, hemicellulose and lignin) of the raw material, lignin is the most difficult to decompose. Its decomposition usually occurs slowly under the whole temperature range used [41]. The TGA result is in agreement with that of ATR-FTIR and NMR.

**Figure 4**

**3.4 Structural Characteristics**

***SEM Analysis***

A close inspection of the raw material and hydrochars by means of scanning electron microscopy technique shown in Figure 5 revealed interesting transformations in the morphologies of the hydrochars vis-a-vis the raw material. The SEM images of the M-PAS$_{200\text{-}20}$ and C-PAS$_{200\text{-}240}$ shown in Figures 5 b and c respectively are alike, and are different from that of the raw material (Figure 5 a). The raw material showed a cellular structure that is characteristic of lignocellulosic materials, while the hydrochars have aggregates of spherical microparticles of about 1–10 μm in diameter. These microparticles originate from the decomposition of cellulose, and the subsequent precipitation and growth into spheres [25]. The lignin component of the raw material on the other hand, probably underwent only partial degradation due to its high thermal stability, producing the rough texture observed in the SEM images of hydrochars [32]. This result implies that the lignocellulosic structure of the raw material was broken during the hydrothermal carbonization process.

**Figure 5**

***Nitrogen Sorption Measurement***

The nitrogen sorption isotherms for the M-PAS$_{200\text{-}20}$ and C-PAS$_{200\text{-}240}$ are shown in Figure 6. Both hydrochars showed characteristics that are representative of Type II isotherms based on the IUPAC system of classification, which is a typical type of isotherm obtained with non-porous materials [42]. It is therefore not surprising that the hydrochars have relatively small BET surface areas (6.1±2.2 $m^2/g$ for M-PAS$_{200\text{-}20}$, and 5.9±1.8 $m^2/g$ for C-PAS$_{200\text{-}240}$) due to the absence of porosity. In such situation the values of the specific surface area calculated only correspond to the external surface [43]. The hydrothermal carbonization process involves carbonization as well as solubilization of the organics, and the formation of tarry substances. The hydrochar produced becomes contaminated with these substances, which block their pores, and make the apparent BET surface area of the hydrochar to be very small [44]. Therefore, improvements of the porosity and the surface area of hydrochars are usually necessary to enable them fit into

specific applications, such as, hydrogen storage or electrical energy storage (supercapacitors) [32].

**Figure 6**

## 4. Conclusion

This article provided some new insights into the similarities between hydrochars prepared from microwave-assisted and conventional hydrothermal carbonization processes of *Prosopis africana* shell, a waste plant material at a low temperature. It is clear from the study that similar transformation can be achieved at 200 °C. The microwave-assisted process proved to be faster in decomposing the waste material as evidenced by the degree of transformation achieved within a short time when compared to the conventional approach. It can therefore be seen, that hydrochar produced for 20 min in the microwave oven exhibited a comparable decomposition pattern to that produced for 240 min in the conventional oven and thus it can be concluded that the materials achieved similar levels of conversion. This work therefore suggests that the microwave-assisted process could have the potential for use in the large-scale production of hydrochars.

## Acknowledgement

We wish to thank the Petroleum Technology Development Fund (PTDF), Nigeria for providing the funding for the PhD studentship of Dr. Sunday E. Elaigwu. We also acknowledge Dr. Mark Lorch and Bob Knight of the Department of Chemistry, University of Hull for providing assistance with the NMR, and CEM microwave oven respectively.

## References

[1] M.M. Titirici, A. Thomas, S.H. Yu, J.O. Muller, M. Antonietti, A direct synthesis of mesoporous carbons with bicontinuous pore morphology from crude plant material by hydrothermal carbonization, Chem. Mater. 19 (2007) 4205-4212.

[2] S.M. Heilmann, H.T. Davis, L.R. Jader, P.A. Lefebvre, M.J. Sadowsky, F.J. Schendel, et al., Hydrothermal carbonization of microalgae, Biomass Bioenerg. 34 (2010) 875-882.

[3] M. Sevilla, A.B. Fuertes, The production of carbon materials by hydrothermal carbonization of cellulose. Carbon 47 (2009) 2281-2289.

[4] I. Pavlovič, Ž. Knez, M. Škerget, Hydrothermal reactions of agricultural and food processing wastes in sub- and supercritical water: A review of fundamentals, mechanisms, and state of research, J. Agric. Food Chem. 61 (2013) 8003–8025.

[5] S.E. Elaigwu, G. Kyriakou, T.J. Prior, G.M. Greenway, Microwave-assisted hydrothermal synthesis of carbon monolith via a soft-template method using resorcinol and formaldehyde as carbon precursor and pluronic F127 as template, Mater. Lett. 123 (2014) 198-201.

[6] M. Nuchter, B. Ondruschka, W. Bonrath, A. Gum, Microwave assisted synthesis - a critical technology overview, Green Chem. 6 (2004) 128-141.

[7] F. Bergius, H. Specht, Die Anwendung hoher Drucke bei chemischen Vorgangen und eine Nachbildung des Entstehungsprozesses der Steinkohle. Wilhelm Knapp Halle ad Saale (1913) 41-58.

[8] M. Guiotoku, C.R. Rambo, F.A. Hansel, W.L.E. Magalhaes, D. Hotza, Microwave-assisted hydrothermal carbonization of lignocellulosic materials, Mater. Lett. 63 (2009) 2707-2709.

[9] M.M. Titirici, M. Antonietti, N. Baccile, Hydrothermal carbon from biomass: a comparison of the local structure from poly- to monosaccharides and pentoses/hexoses, Green Chem. 10 (2008) 1204-1212.

[10] M. Antonietti, M.M. Titirici, Coal from carbohydrates: The "chimie douce" of carbon, Cr Chim. 13 (2010) 167-173.

[11] S.H. Yu, B. Hu, K. Wang, L.H. Wu, M. Antonietti, M.M. Titirici, Engineering

carbon materials from the hydrothermal carbonization process of biomass, Adv. Mater. 22 (2010) 813-828.

[12] S.K. Hoekman, A. Broch, C. Robbins, Hydrothermal carbonization (HTC) of lignocellulosic biomass, Energ. Fuel 25 (2011) 1802-1810.

[13] N. Baccile, G. Laurent, C. Coelho, F. Babonneau, L. Zhao, M.M. Titirici, Structural insights on nitrogen-containing hydrothermal carbon using solid-state magic angle spinning $^{13}C$ and $^{15}N$ nuclear magnetic resonance, J. Phys Chem. C 115 (2011) 8976-8982.

[14] J.D. Mao, X.Y. Cao, K.S. Ro, M. Chappell, Y.A. Li, Chemical structures of swine-manure chars produced under different carbonization conditions investigated by advanced solid-state $^{13}C$ nuclear magnetic resonance (NMR) spectroscopy, Energ. Fuel 25 (2011) 388-397.

[15] E. Sabio, A. Álvarez-Murillo, S. Román, B. Ledesma, Conversion of tomato-peel waste into solid fuel by hydrothermal carbonization: Influence of the processing variables, Waste Manage (2015) http://dx.doi.org/10.1016/j.wasman.2015.04.016

[16] O.O.D. Afolabi, M. Sohail, C.P.L. Thomas, Microwave hydrothermal carbonization of human biowastes, Waste Biomass Valor 6 (2015) 147-157.

[17] J.F.R. Flora, X. Lu, L. Li, J.R.V. Flora, N.D. Berge, The effects of alkalinity and acidity of process water and hydrochar washing on the adsorption of atrazine on hydrothermally produced hydrochar, Chemosphere 93 (2013) 1989–1996.

[18] S.E. Elaigwu, V. Rocher, G. Kyriakou, G.M. Greenway, Removal of $Pb^{2+}$ and $Cd^{2+}$ from aqueous solution using chars from pyrolysis and microwave-assisted hydrothermal carbonization of *Prosopis africana* shell, J. Ind. Eng. Chem. 20 (2014) 3467-3473.

[19] Q. Xu, Q. Qian, A. Quek, N. Ai, G. Zeng, J. Wang, Hydrothermal carbonization of macroalgae and the effects of experimental parameters on the properties of hydrochars, ACS Sustainable Chem. Eng. 1 (2013) 1092–1101.

[20] Y. Gao, X. Wang, J. Wang, X. Li, J. Cheng, H. Yang, et al., Effect of residence time on chemical and structural properties of hydrochar obtained by hydrothermal carbonization of water hyacinth, Energy 58 (2013) 376-383.

[21] O. Mašek, V. Budarin, M. Gronnow, K. Crombie, P. Brownsort, E. Fitzpatrick, P. Hurst, Microwave and slow pyrolysis biochar-Comparison of physical and functional properties, J. Anal. Appl. Pyrol. 100 (2013) 41-48.

[22] V.L. Budarin, J.H. Clark, B.a. Lanigan, P. Shuttleworth, D.J. Macquarrie, Microwave assisted decomposition of cellulose: a new thermochemical route for biomass exploitation, Bioresource Technol. 101 (2010) 3776-3779.

[23] A. Kruse, A. Gawlik, Biomass Conversion in Water at 330-410 °C and 30-50 MPa. Identification of key compounds for indicating different chemical reaction pathways, Ind. Eng. Chem. Res. 42 (2003) 267-279.

[24] M. Möller, P. Nilges, F. Harnisch, U. Schröder, Subcritical water as reaction environment: Fundamentals of hydrothermal biomass transformation, ChemSusChem 4 (2011) 566-579.

[25] M. Sevilla, J.A. Macia-Agullo, A.B. Fuertes, Hydrothermal carbonization of biomass as a route for the sequestration of $CO_2$: chemical and structural properties of the carbonized products, Biomass Bioenerg. 35 (2011) 3152-3159.

[26] C. Falco, N. Baccile, M.M. Titirici, Morphological and structural differences between glucose, cellulose and lignocellulosic biomass derived hydrothermal carbons, Green Chem. 13 (2011) 3273-3281.

[27] S. Kang, X. Li, J. Fan, J. Chang, Characterization of hydrochars produced by hydrothermal carbonization of lignin, cellulose, d-xylose, and wood meal, Ind. Eng. Chem. Res. 51 (2012) 9023-9031.

[28] N.D. Berge, K.S. Ro, J. Mao, J.R.V. Flora, M.A. Chappell, S. Bae, Hydrothermal carbonization of municipal waste streams, Environ. Sci. Technol. 45 (2011) 5696-5703.

[29] Z. Liu, F.S. Zhang, J. Wu, Characterization and application of chars produced from pinewood pyrolysis and hydrothermal treatment, Fuel 89 (2010) 510-514.

[30] E. Erdogan, B. Atila, J. Mumme, M.T. Reza, A. Toptas, M. Elibol, J. Yanik, Characterization of products from hydrothermal carbonization of orange pomace including anaerobic digestibility of process liquor, Bioresource Technol. 196 (2015) 35-42.

[31] M.T. Reza, M.H. Uddin, J.G. Lynam, S.K. Hoekman, C.J. Coronella, Hydrothermal carbonization of loblolly pine: reaction chemistry and water balance, Biomass Conv. Bioref. 4 (2014) 311-321.

[32] G.K. Parshetti, S.K. Hoekman, R. Balasubramanian, Chemical, structural and combustion characteristics of carbonaceous products obtained by hydrothermal carbonization of palm empty fruit bunches, Bioresource Technol. 135 (2013) 683-689.

[33] M.H. Thomsen, A. Thygesen, A.B. Thomsen, Hydrothermal treatment of wheat straw at pilot plant scale using a three-step reactor system aiming at high hemicellulose recovery, high cellulose digestibility and low lignin hydrolysis, Bioresource Technol. 99 (2008) 4221-4228.

[34] S.V. Vassilev, D. Baxter, L.K. Andersen, C.G. Vassileva, T.J. Morgan, An overview of the organic and inorganic phase composition of biomass, Fuel 94 (2012) 1-33.

[35] Z. Liu, A. Quek, S.K. Hoekman, R. Balasubramania, Production of solid biochar fuel from waste biomass by hydrothermal carbonization, Fuel 103 (2013) 943-949.

[36] M.M. Titirici, R. Demir-Cakan, N. Baccile, M. Antonietti, Carboxylate-rich carbonaceous materials via one-step hydrothermal carbonization of glucose in the presence of acrylic acid, Chem. Mater. 21 (2009) 484-490.

[37] N. Baccile, G. Laurent, F. Babonneau, F. Fayon, M.M. Titirici, M. Antonietti, Structural characterization of hydrothermal carbon spheres by advanced solid-state MAS $^{13}C$ NMR investigations, J. Phys. Chem. C 113 (2009) 9644-9654.

[38] J. Mao, K.M. Holtman, J.T. Scott, J.F. Kadla, K. Schmidt-Rohr, Differences between lignin in unprocessed wood, milled wood, mutant wood, and extracted lignin detected by $^{13}C$ solid-state NMR, J. Agric. Food Chem. 54 (2006) 9677-9686.

[39] M.A. Islam, G. Kabir, M. Asif, B.H. Hameed, Combustion kinetics of hydrochar produced from hydrothermal carbonisation of Karanj (*Pongamia pinnata*) fruit hulls via thermogravimetric analysis, Bioresource Technol. 194 (2015) 14–20.

[40] M. Lapuerta, J.J. Hernandez, J. Rodriguez, Kinetics of devolatilisation of forestry wastes from thermogravimetric analysis, Biomass Bioenerg. 27 (2004) 385-391.

[41] H. Yang, R. Yan, H. Chen, D. Lee, C. Zheng, Characteristics of hemicellulose, cellulose and lignin pyrolysis, Fuel 86 (2007) 1781-1788.

[42] K.S.W. Sing, D.H. Everett, R.A.W. Haul, L. Moscou, R.A. Pierotti, J. Rouquerol, et al., Reporting physisorption data for gas/solid systems, Pure Appl. Chem. 57 (1985) 603-619.

[43] A.B. Fuertes, M.C. Arbestain, M. Sevilla, J.A. Maciá-Agulló, S. Fiol, R. López, et al., Chemical and structural properties of carbonaceous products obtained by pyrolysis and hydrothermal carbonisation of corn stover, Aust. J. Soil Res. 48 (2010) 618-626.

[44] K. Mochidzuki, N. Sato, A. Sakoda, Production and characterization of carbonaceous adsorbents from biomass wastes by aqueous phase carbonization, Adsorption 11 (2005) 669-673.

## Tables

| Materials | Yields (%) | C (%) | H (%) | N (%) | O[a] (%) | O/C * | H/C* | pH | Ash (%) | HHV (MJ $kg^{-1}$) | Energy densification ratio |
|---|---|---|---|---|---|---|---|---|---|---|---|
| *P. africana* shell | | 46.58±0.01 | 6.94±0.04 | 1.57±0.09 | 44.91±0.10 | 0.73 | 1.77 | 5.34±0.02 | 3.77±1.13 | 17.64 | |
| **M-PAS** | | | | | | | | | | | |
| $M\text{-}PAS_{200\text{-}20}$ | 30.60±2.13 | 58.08±1.12 | 6.18±0.80 | 1.61±0.01 | 34.13±0.31 | 0.44 | 1.27 | 4.05±0.03 | 9.32±0.50 | 22.37 | 1.27 |
| $M\text{-}PAS_{200\text{-}15}$ | 32.21±1.55 | 55.81±0.06 | 6.61±0.09 | 1.60±0.01 | 35.98±0.14 | 0.48 | 1.41 | 4.21±0.01 | 9.05±0.45 | 21.88 | 1.24 |
| $M\text{-}PAS_{200\text{-}10}$ | 33.01±0.98 | 55.69±0.00 | 6.67±0.03 | 1.57±0.02 | 36.07±0.05 | 0.49 | 1.43 | 4.37±0.01 | 9.10±0.10 | 21.91 | 1.24 |
| $M\text{-}PAS_{200\text{-}5}$ | 36.37±2.01 | 55.46±0.08 | 6.71±0.05 | 1.48±0.00 | 36.35±0.06 | 0.49 | 1.44 | 4.51±0.00 | 8.72±0.85 | 21.84 | 1.24 |
| **C-PAS** | | | | | | | | | | | |
| $C\text{-}PAS_{200\text{-}240}$ | 30.85±0.53 | 57.86±1.10 | 6.37±0.06 | 1.46±0.05 | 34.31±1.21 | 0.44 | 1.31 | 4.34±0.01 | 9.25±0.45 | 22.53 | 1.28 |
| $C\text{-}PAS_{200\text{-}180}$ | 34.78±0.04 | 53.85±1.02 | 6.53±0.01 | 1.47±0.05 | 38.15±0.96 | 0.53 | 1.44 | 4.41±0.02 | 9.01±0.32 | 20.72 | 1.18 |
| $C\text{-}PAS_{200\text{-}120}$ | 37.87±0.20 | 51.25±0.90 | 6.72±0.02 | 1.65±0.03 | 40.38±0.95 | 0.59 | 1.56 | 4.57±0.01 | 8.87±0.75 | 19.72 | 1.12 |

**[a] The oxygen content was determined by difference [100% - (C%+H%+N%)] [8]**

*** Atomic ratios**

**Table 1: Product yields, CHN analysis, pH, ash contents and energy properties of the raw *Prosopis africana* shell and hydrochars from microwave-assisted and conventional hydrothermal carbonization processes**

## Figures

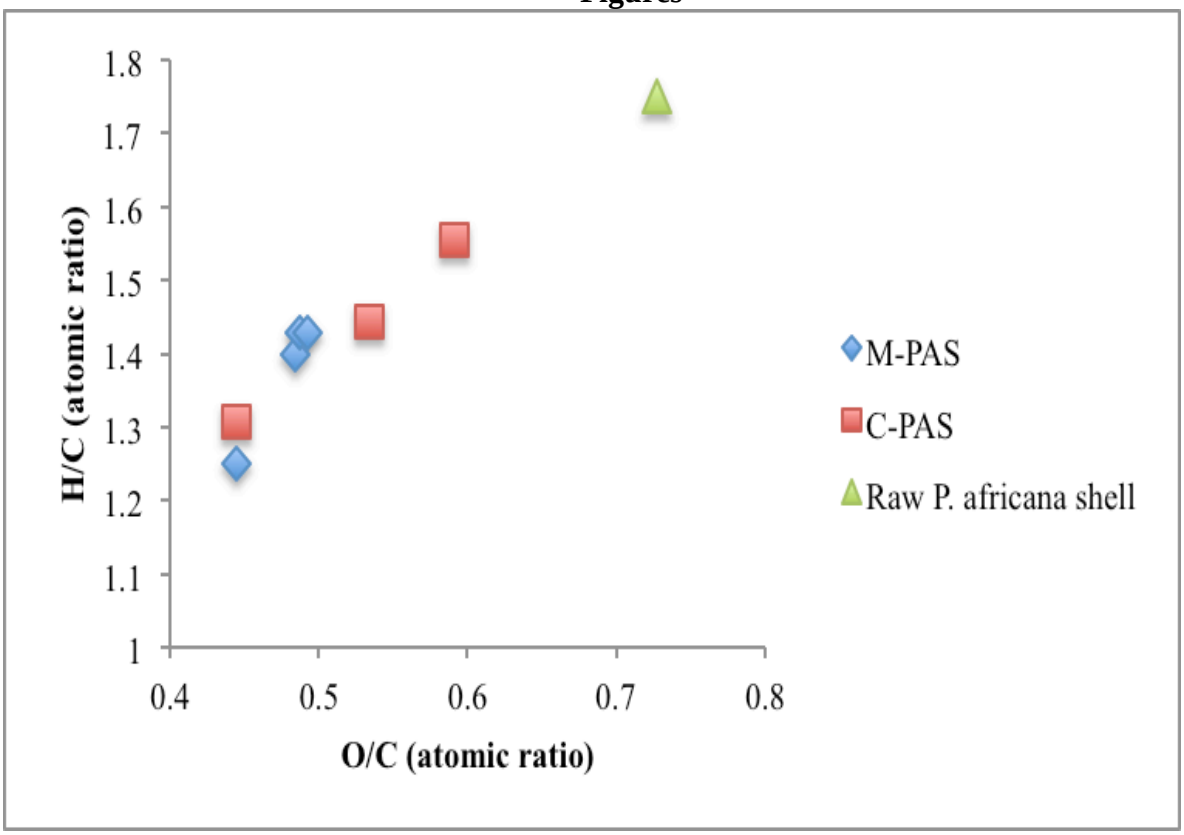


**Figure 1**

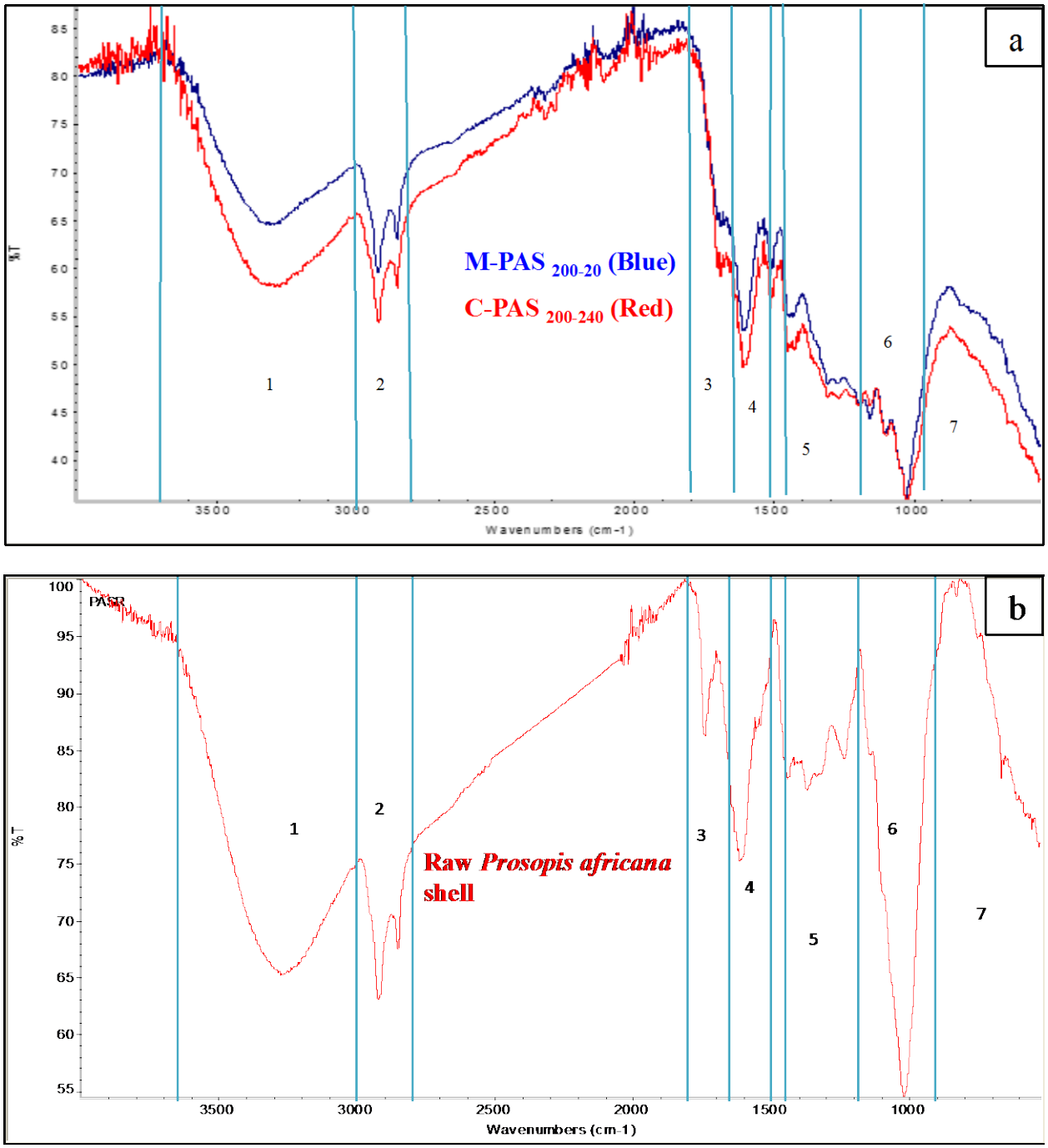


**Figure 2**

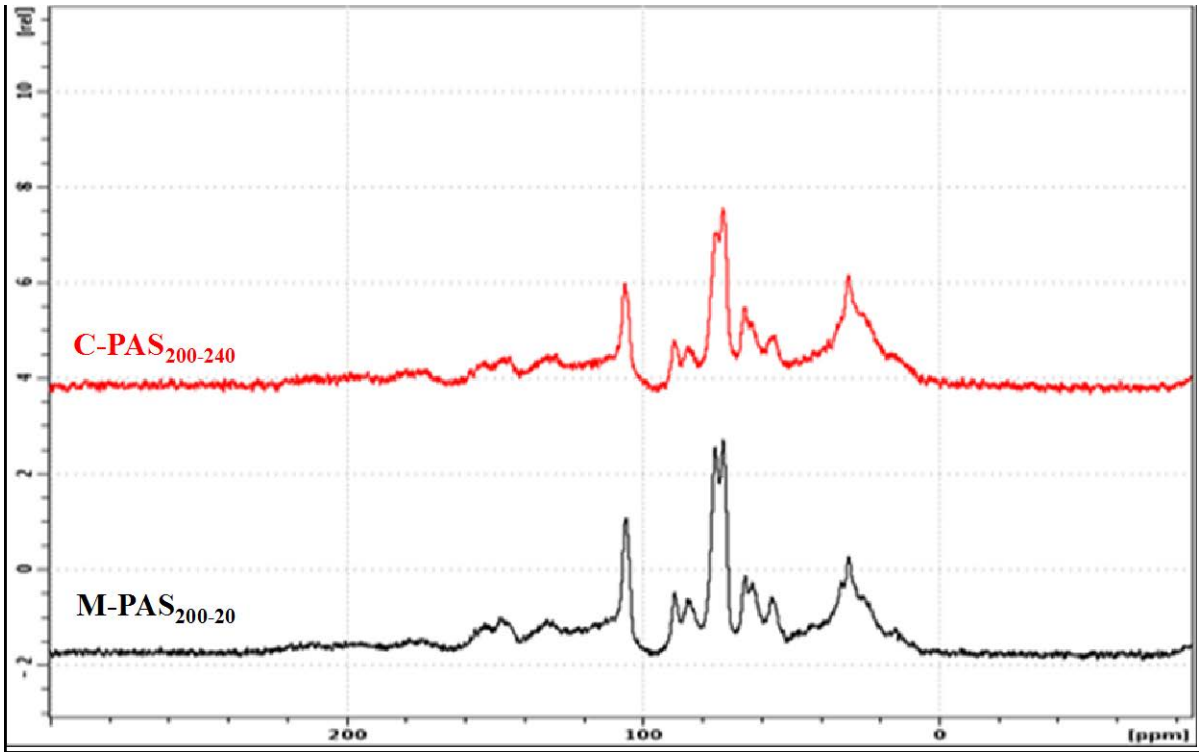


**Figure 3**

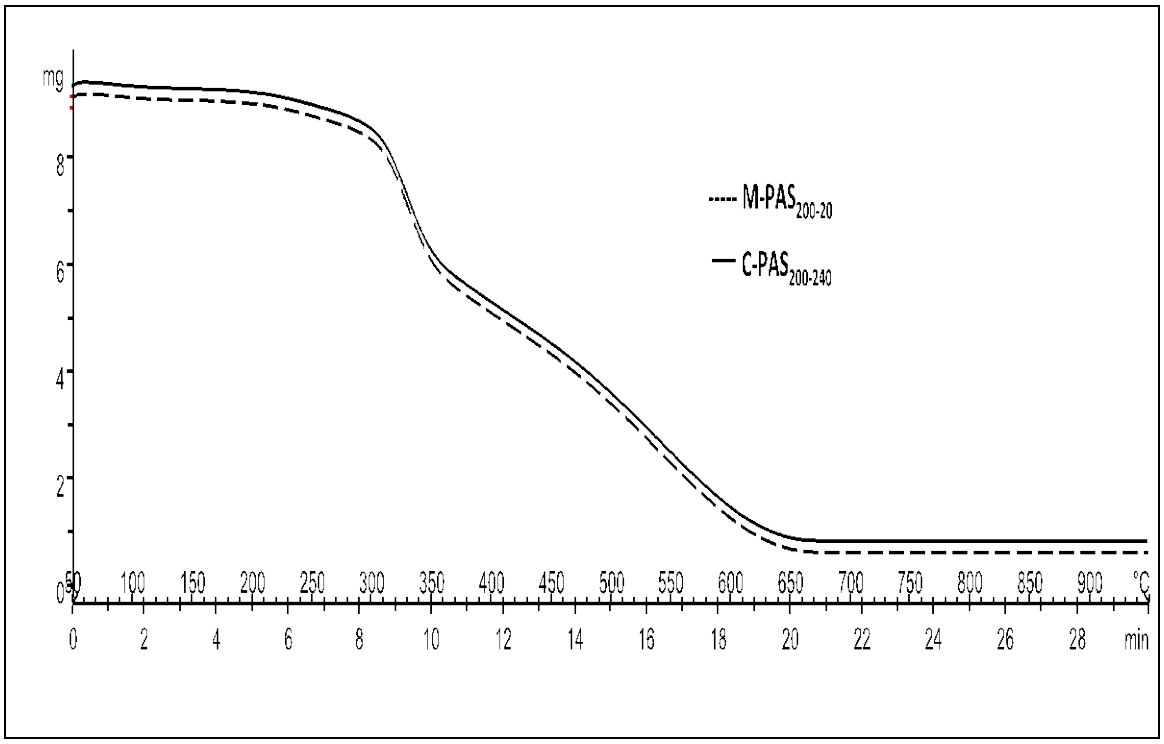


**Figure 4**

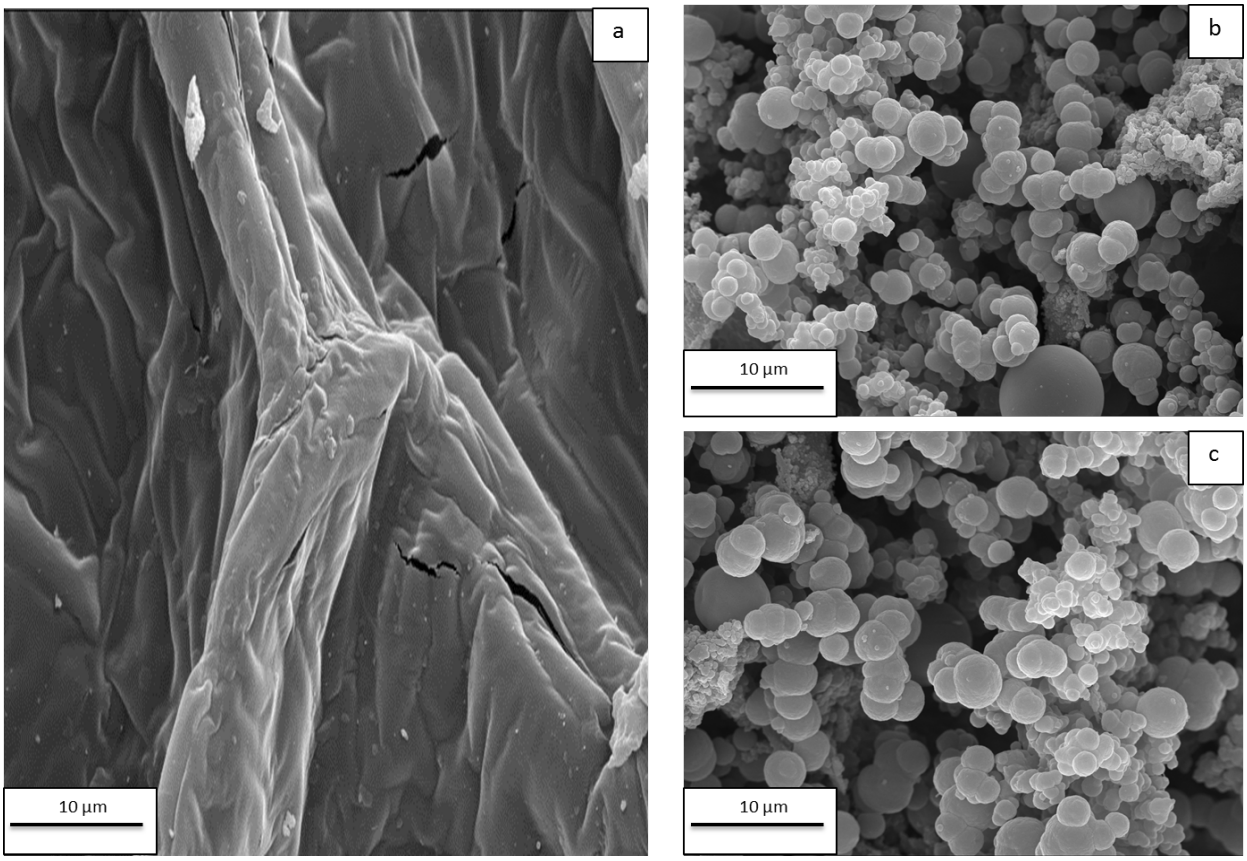


**Figure 5**

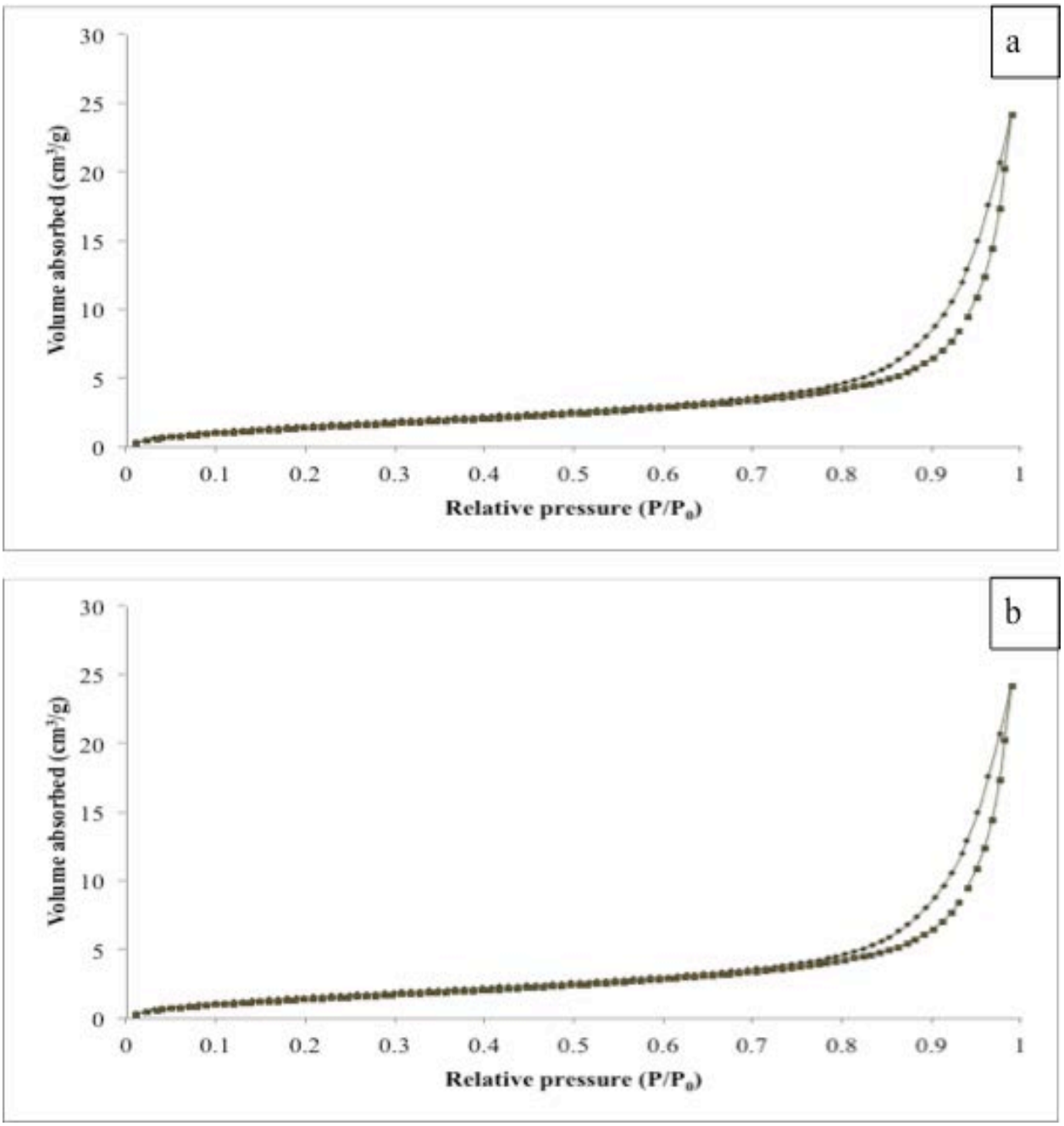


**Figure 6**